DOI: 10.1002/JLB.4A0419-123R

JLB JOURNAL OF LEUKOCYTE BIOLOGY

ARTICLE

Sensitivity of Kupffer cells and liver sinusoidal endothelial cells to ricin toxin and ricin toxin–Ab complexes

Bridget Mooney | **Fernando J. Torres-Velez** | **Jennifer Doering** | **Dylan J. Ehrbar** | **Nicholas J. Mantis**

Division of Infectious Diseases, Wadsworth Center, New York State Department of Health, Albany, New York, USA

Correspondence
Nicholas J. Mantis, Division of Infectious Diseases, Wadsworth Center, New York State Department of Health, 120 New Scotland Ave, Albany, NY 12208, USA.
Email: nicholas.mantis@health.ny.gov

Abstract

Ricin toxin is a plant-derived, ribosome-inactivating protein that is rapidly cleared from circulation by Kupffer cells (KCs) and liver sinusoidal endothelial cells (LSECs)—with fatal consequences. Rather than being inactivated, ricin evades normal degradative pathways and kills both KCs and LSECs with remarkable efficiency. Uptake of ricin by these 2 specialized cell types in the liver occurs by 2 parallel routes: a "lactose-sensitive" pathway mediated by ricin's galactose/N-acetylgalactosamine-specific lectin subunit (RTB), and a "mannose-sensitive" pathway mediated by the mannose receptor (MR; CD206) or other C-type lectins capable of recognizing the mannose-side chains displayed on ricin's A (RTA) and B subunits. In this report, we investigated the capacity of a collection of ricin-specific mouse MAb and camelid single-domain (V_HH) antibodies to protect KCs and LSECs from ricin-induced killing. In the case of KCs, individual MAbs against RTA or RTB afforded near complete protection against ricin in ex vivo and in vivo challenge studies. In contrast, individual MAbs or V_HHs afforded little (<40%) or even no protection to LSECs against ricin-induced death. Complete protection of LSECs was only achieved with MAb or V_HH cocktails, with the most effective mixtures targeting RTA and RTB simultaneously. Although the exact mechanisms of protection of LSECs remain unknown, evidence indicates that the Ab cocktails exert their effects on the mannose-sensitive uptake pathway without the need for Fcγ receptor involvement. In addition to advancing our understanding of how toxins and small immune complexes are processed by KCs and LSECs, our study has important implications for the development of Ab-based therapies designed to prevent or treat ricin exposure should the toxin be weaponized.

KEYWORDS
biodefense, c-type lectin, toxin

1 | INTRODUCTION

Ricin toxin has been classified as a biological threat agent by the Centers for Disease Control and Prevention because of its extreme toxicity, the ease by which it can be procured from castor beans, and the absence of any available countermeasures.[1] Continued concerns about ricin are underscored by a recent NATO Biomedical Advisory Council report that ranked ricin at the top of its list of agents with weaponization potential.[2] Ricin is a ~65 kDa heterodimeric glycoprotein consisting of 2 subunits, RTA and RTB, which are joined via a single disulfide bond. RTB (262 amino acid residues), a bivalent lectin that recognizes galactose (Gal) and N-acetyl galactosamine (GalNAc), promotes ricin attachment to membrane bound glycoproteins and glycolipids on mammalian cells. RTB also facilitates transport of ricin from the plasma membrane to the trans-Golgi network (TGN) and endoplasmic reticulum (ER), where RTA is liberated from RTB and translocated into the cytoplasm. RTA (267 amino acid residues) catalyzes the hydrolysis of the sarcin/ricin loop of 28S ribosomal RNA, thereby arresting protein synthesis and triggering programmed cell

Abbreviations: BDMCs, bone marrow-derived macrophages; ER, endoplasmic reticulum; GBSS, Gey's balanced salt solution; Gal, galactose; GalNAc, N-acetyl galactosamine; KCs, Kupffer cells; LSECs, liver sinusoidal endothelial cells; PI, propidium iodide; TGN, trans-Golgi network.

Received: 9 April 2019 | Revised: 3 June 2019 | Accepted: 2 July 2019

death pathways.[3–5] Because the addition of exogenous lactose inhibits RTB-mediated attachment to host cells, this pathway is referred to as a "lactose-sensitive" pathway.[6]

Ricin can also gain entry into certain cells types through a "mannose-sensitive" pathway that was first described on bone marrow-derived macrophages (BDMCs) and later shown to exist on Kupffer cells (KCs) and liver sinusoidal endothelial cells (LSECs).[6–10] Ricin is mannosylated at 3 different asparagine residues; 1 on RTA (position 95) and 2 on RTB (positions 135 and 280).[11–13] A number of studies have implicated the mannose receptor (MR:CD206) as being responsible for ricin uptake into BDMC, KCs, and LSECs, although most of those studies were conducted years before the full suite of the C-type lectins (CTL) and their roles in pathogen recognition were discovered.[14] Nonetheless, the mannose-sensitive pathway is a highly efficient route by which ricin enters and kills in KCs and LSECs, due in part to increased rates of internalization, as compared with the lactose-sensitive uptake pathway.[8–10]

In this report, we sought to revisit the sensitivity of KCs and LSECs to ricin in light of efforts to develop MAb-based therapies and prophylactics for ricin exposure.[15–18] For example, we recently demonstrated that i.v. delivery of a single MAb, PB10, directed against RTA was able to rescue Rhesus macaques from lethal dose aerosol challenge if administered within a 4 h window.[17] In that model, ricin intoxication is largely restricted to the lung with little systemic involvement.[19] In contrast, following injection, ricin homes to the liver where it concentrates in KCs and LSECs.[8–10,20–24] Roche and colleagues reported in a mouse model that a protective anti-RTA MAb was beneficial in blunting liver damage following ricin exposure, although the specific interactions between KCs and LSECs were not investigated. LSECs are of particular interest in this regard considering their importance in scavenging mannosylated proteins from circulation[25,26] coupled with their central role in promoting the clearance of small immune complexes (SICs) from blood.[27,28]

2 | MATERIALS AND METHODS

2.1 | Chemicals and biologic reagents

Ricin toxin (*Ricinus communis* agglutinin II) was purchased from Vector Laboratories (Burlingame, CA) and was dialyzed to remove sodium azide, as described.[29] Native RTA from *R. communis* seeds was obtained from BEI Resources (Catalog NR-2619; Manassas, VA).[30] HEPES buffer consisted of 0.22 g/L KCl, 7.7 g/L NaCl, 0.14 g/L Na_2HPO_4, 1.8 g/L D-glucose, 7.15 g/L HEPES, and 0.001 g/L phenol red in distilled water. Gey's balanced salt solution (GBSS) contained 0.220 g $CaCl_2{\cdot}2H_2O$, 0.370 g/L KCl, 0.030 g/L KH_2PO_4, 0.210 g/L $MgCl_2.6H_2O$, 0.070 g/L $MgSO_4{\cdot}7H_2O$, 8.00 g/L NaCl, 0.227 g/L $NaHCO_3$, 0.120 g/L Na_2HPO_4, and 1.00 g/L D-glucose in distilled water. MACS buffer consisted of 0.5% (w/v) BSA and 2 mM EDTA in PBS without Ca^{2+} and Mg^{+} (Thermo Fisher, Waltham, MA). Staining/wash buffer (SWB) for flow cytometry contained 2% (v/v) FBS (Thermo Fisher) in PBS.

2.2 | MAbs and V_HHs

The MAbs used in this study are shown in Supplemental Table S1. The MAbs were purified from hybridoma supernatants by Protein A chromatography at the Dana Farber Cancer Institute (DFCI) Monoclonal Antibody Core facility (Boston, MA).[31] The murine MAbs against RTA (SyH7, PA1, IB2, WECB2, JD4, and PB10) and RTB (MH3, SylH3, LC5, 24B11, 8B3, and 8A1) have been previously described.[29,31–35] The V_HHs against RTA (JIVF5, V5E1, V1D3, and V13G5) and RTB (JIZB7, V5D1) have also been described, except for V11E10 (manuscript in preparation).[36–39]

2.3 | Cell lines and primary cell culture

The macrophage cell line, J774E, originally obtained from Dr. Philip Stahl, Washington University School of Medicine (St Louis, MO), was cultured in DMEM containing 10% (v/v) FBS and was used between passage numbers 6 and 12.[6] Primary KCs were cultured in medium comprised of DMEM, 10% (v/v) heat-inactivated FBS, 100 U/ml penicillin, 100 μg/ml streptomycin, 2 mM L-glutamine, 10 μg/ml insulin, and 50 μM 2-mercaptoethanol. Isolated and purified LSECs were cultured in medium containing 44% (v/v) MCDB 131 media (Sigma–Aldrich, St. Louis, MO), 10% heat-inactivated FBS, 100 U/ml penicillin, 100 μg/ml streptomycin, 2 mM L-glutamine, 1 ng/ml dexamethasone, and 44% (v/v) endothelial cell growth medium-2 microvascular (EGM-2MV) containing SingleQuots™ (Lonza, Walkersville, MD). All cells were cultured on 0.1 mg/ml collagen-coated plates. Plates were coated by adding the collagen solution to the wells for 1 h at RT, removing, and rinsing 1 time with calcium and magnesium free PBS. Coated plates were stored for up to 1 month at 4°C. All cells were kept in a humidified incubator at 37°C and 5% atmospheric CO_2.

2.4 | Isolation of primary murine KCs and LSECs

Liver perfusions were performed on female Swiss Webster mice 7–12 weeks of age, purchased from Taconic Biosciences (Rensselaer, NY). The mice were kept in a specific-pathogen free environment and treated in accordance to Wadsworth Center's Institutional Animal Care and Use Committee guidelines. Mice were euthanized by CO_2 asphyxiation followed by cervical dislocation. For the liver perfusion, the inferior vena cava was cannulated with a 24G x 0.75 in closed IV Catheter System with Single Port (BD Bioscience, Franklin Lakes, NJ) connected to a 20-cc syringe. A total of 20 ml preperfusion buffer composed of GBSS without calcium (37°C) was applied with a peristaltic pump (KD Scientific, Holliston, MA) at a flow rate of 5 ml/min. The hepatic portal vein was clipped to allow for fluid drainage. For the enzymatic digestion, 10 ml of 37°C perfusion buffer consisting of GBSS with calcium and 0.0008 g/ml Type IV Collagenase (Thermo Fisher) was pumped through the liver at 5 ml/min. Following digestion, the liver was excised, and the gall bladder was removed before it was placed in a 60 × 15 mm cell culture dish containing 10 ml of 0.1% (w/v) BSA (Thermo Fisher) in PBS without Ca^{2+} and Mg^{+} (BSA–PBS). In a sterilization hood at room temperature, primary parenchymal and nonparenchymal liver cells were removed from the liver by gentle

tearing and shaking. The cell suspension was poured through a 100 μm filter into a 50-ml conical tube. This step was repeated until no more cells were released and the conical tube was filled to a total volume of 40 ml with BSA–PBS. The cell suspension was subject to centrifugation at 50*g* for 3 min 2 times to remove parenchymal cells, and the supernatants containing nonparenchymal cells were stored on ice. All subsequent steps were performed at 4°C. The nonparenchymal cells were pelleted by centrifuging at 800*g* for 10 min and the RBCs were lysed by incubating with 7 ml ammonium chloride (Stemcell Technologies, Vancouver, Canada) for 4 min. The RBC lysate was removed by adding 23 ml of BSA–PBS and centrifuging for 5 min at 800*g*.

2.5 | Density gradient centrifugation and MACS

Following parenchymal cell and RBC removal, nonparenchymal cells were resuspended in 5 ml of 17.6% (w/v) Optiprep™ (Cosmo Bio USA, Carlsbad, CA) in a 15-ml conical tube. A 5-ml layer of 8.2% (w/v) Optiprep™ was gently layered on top. Cells were centrifuged at 1400*g* for 17 min. without brake at 4°C. Cells at the interface between both layers (~2–3 ml total volume) were carefully removed and placed in a 50-ml conical tube. BSA–PBS was added to a final volume of 30 ml, and the cells were pelleted at 800*g* for 5 min. Cells were resuspended in 170 μl of degassed MACS buffer, and 30 μl of anti-F4/80 microbeads (Miltenyi Biotec, Auburn, CA) were added to positively select for KCs. The cells and beads were incubated for 20 min at 4°C in the dark. Cells were washed twice with 1 ml MACS buffer and resuspended in 0.5 ml MACS buffer. Cells were separated using a MiniMACS™ kit (Miltenyi Biotec). In the presence of a magnetic field, the column was hydrated with 0.5 ml of MACS buffer, the cell suspension was added, and the column was rinsed 3× with 0.5 ml of MACS buffer. The eluted or negatively selected cells were collected in a 15-ml conical tube, and the positively selected cells were retrieved by removing the column from the magnetic field, adding 1 ml of MACS buffer, and plunging into a 15-ml conical tube. Cells were seeded on collagen-coated plates, and images were gathered with a phase contrast microscope.

2.6 | Flow cytometry

Cells were seeded in a clear, U-bottom, 96-well plate at a density of 1×10^7 cells/ml (0.1 ml per well). Controls included unstained cells and individually stained cells. For KC and LSEC purity assessment, cells were pelleted by centrifugation (400g for 5 min) and resuspended in 100 μl Fc blocking solution containing TruStain fcXTM (anti-mouse CD16/32) antibody (Biolegend, San Diego, CA) diluted to 1:500 in SWB. Cells were incubated on ice for 15 min in blocking solution and centrifuged at 400g for 5 min. Cells were incubated with 100 μl of conjugated primary antibodies diluted in SWB (Supplemental Table S2) on ice for 30–45 min. For FITC-ricin binding studies, cells were incubated on ice for 30 min with either FITC-ricin alone (3 μg/ml), FITC-ricin and lactose (0.1 M), FITC-ricin and mannan (10 mg/ml), or FITC-ricin and mannan and lactose. Plates were centrifuged at 400g for 5 min, and the cells were washed twice in 200 μl of SWB. Finally, the plate was spun at 880g for 5 min, and the cells were resuspended in 400 μl of SWB in 5 ml Falcon tubes. Cells were analyzed immediately with a BD FACSCalibur™ flow cytometer (BD Biosciences). Cell viability was assessed by adding 5 μl of the propidium iodide (PI) staining solution from a FITC Annexin V Apoptosis Detection Kit II (BD Pharmingen, San Diego, CA) to the unstained control.

2.7 | Ricin cytotoxicity and neutralization assays

White, flat-bottom 96-well plates were coated with Type I rat tail collagen (0.1 mg/ml; Thermo Fisher Scientific) diluted in PBS. For ricin toxin dose optimization, LSECs and J774E cells were seeded at 2×10^5, 5×10^5, and 1×10^6 cells/ml, and KCs were seeded at 1×10^5, 2×10^5, and 5×10^5 cells/ml. Cells were treated with ricin diluted 2-fold starting at 100 ng/ml for 18 h. At this point, the ricin was removed, the cells were washed with HEPES buffer, and regular media was placed in the well. After 24 h, cell viability was assessed using CellTiter-GLO reagent (Promega, Madison, WI) and a Spectramax L Microplate Reader (Molecular Devices, Sunnyvale, CA). For the 2 h pulse ricin treatment, cells were treated with ricin diluted 2-fold starting at 400 ng/ml right after an 18 h attachment period, and cell viability was assessed 24 h later. For plant-based RTA treatment, cells were seeded at 5×10^5 cells/ml and treated overnight with RTA diluted 2-fold starting at 400 ng/ml. All treatments were performed in triplicate, and 100% viability was defined as the average value obtained from wells in which cells were treated solely with cell medium.

The ricin toxin neutralization assays with murine MAbs and V_HHs followed an 18 h treatment time-course incorporating ricin at a dose corresponding to the EC_{90} from the ricin cytotoxicity curves: LSECs and J774E cells were treated with 10 ng/ml of ricin, and KCs were treated with 1 ng/ml of ricin. The MAbs were titrated into the wells containing ricin starting at 20 μg/ml. As a positive control, cells were treated with pooled antisera from BALB/c mice that had been hyperimmunized with RiVax.[40] Dose response curves for all 3 cell types were also generated for this antiserum in the presence of ricin. Cell viability was assessed as described above. Cell viability was normalized to cells treated with medium only, and background noise was reduced by subtracting the average of wells treated only with ricin at a dose equivalent to the EC_{90} value.

2.8 | MR and LSECtin binding assays

Immulon 4HBX flat bottom microtiter plates (Thermo Scientific, Rochester, NY) were coated overnight at 4°C with ricin (1 μg/ml), washed with PBS plus 0.05% (v/v) Tween-20 (PBS-T), then blocked for 2 h with PBS-T containing 2% (v/v) goat serum (Gibco, Gaithersburg, MD). Samples were prepared in a separate PVC plate. Ten-fold serial dilutions of 0.1 M mannan (Sigma–Aldrich) were mixed with recombinant mouse MR (R&D Systems, Minneapolis, MN) or LSECtin (R&D Systems) at concentrations equivalent to their relative EC_{90} values (~10 μg/ml). The mannan-MR or LSECtin mixtures were incubated for 1 h at RT and then applied to the microtiter plate coated with ricin, in duplicate, and incubated for 1 h. Control wells contained only MR. Plates were then washed and probed with HRP-conjugated anti-His

tag (R&D Systems) for 45 min and developed. For inhibition assays, 5-fold serial dilutions of MAbs (starting at 500 μg/ml for PB10 or SyH7 separately, 250 μg/ml of each when combined) were mixed with recombinant mouse MR, incubated for 1 h at RT and then applied to the microtiter plate coated with ricin, as described above.

2.9 | Lactose and mannan inhibition studies

Based on cytotoxicity results for the 2 h pulse treatment with ricin toxin, cells were seeded at 5×10^5 cells/ml in collagen-coated 96-well plates and were treated with ricin at a dose approximately equal to the EC_{90} value on the ricin dose curves. Approximately 18 h after seeding, LSECs and KCs were treated with 50 ng/ml of ricin, and J774E cells were treated with 100 ng/ml of ricin for 2 h. Concurrently, cells were treated with either 1 mg/ml of yeast α-mannan (Sigma–Aldrich), 0.1 M lactose (Thermo Fisher), or a mixture of yeast α-mannan and lactose. Cell viability was assessed 24 h later using CellTiter-GLO reagent and a Spectramax L Microplate reader. Cell viability was normalized to cells treated with medium only and background noise was reduced by subtracting the average of wells treated only with ricin at a dose equivalent to the EC_{90} value.

2.10 | In vivo ricin toxin neutralization assays

Mice were challenged i.p. with 0.6 μg or i.v. with 2 μg ricin toxin in PBS premixed with 20 μg of total MAb(s). Controls included mice treated solely with ricin toxin or PBS. After 18 h, the livers were perfused, and the cells were separated down to a KC/LSEC mixture using density gradient centrifugation, as described above. Flow cytometry was performed on this mixture to assess KC depletion in each treatment group. During the same experiments, livers and spleens were harvested for further analysis using immunohistochemistry (IHC).

2.11 | Immunohistochemistry

Tissues were immersed and allowed to fix in 10% buffered formalin for 24 h, and subsequently transferred to 70% ethanol prior to processing and embedding. Tissue sections were stained with hematoxylin and eosin for histopathologic evaluation. Tissue sections, 3–4 μm in thickness, were deparaffinized in CitriSolve (Decon Labs., King of Prussia, PA) and rehydrated by processing through graded alcohols. For F4/80 staining, antigen retrieval was performed by treating tissue sections with Proteinase K (0.1 mg/ml) for 5 min at room temperature. Antigen retrieval for cleaved caspase-3 was performed by heating the slides to 95°C in Rodent Decloaker, a citrate-based solution (Biocare Medical, Pacheco, CA) for 40 minutes using a rice steamer. For both procedures, endogenous IgG and nonspecific background were blocked with Rodent Block M (Biocare Medical), followed by an alkaline phosphatase block (BLOXALL; Vector Laboratories). For F4/80 staining, primary Ab (GTX26640; GeneTex, Irvine, CA) was incubated on tissue sections at a 1:100 dilution for 1 h at room temperature. Subsequently, sections were sequentially incubated with a rat-on-rodent tissue HRP-based polymer (Biocare Medical) and Vina Green chromogen (Biocare Medical). For caspase-3 staining, the primary Ab (GTX22302; Gene Tex, Irvine, CA) was incubated on the tissue sections at a dilution of 1:100 for 1 h at room temperature. Subsequently, sections were sequentially incubated with a rabbit-on-rodent tissue alkaline phosphatase-based polymer (Biocare Medical) containing blocking reagent (XM Factor, Biocare Medical), and fast red (Warp Red; Biocare Medical). For both procedures, sections were counterstained with Tacha's hematoxylin (Biocare Medical) and mounted using a permanent mounting medium (EcoMount; Biocare Medical).

2.12 | Statistical analysis

Statistical analysis was carried out with GraphPad Prism 7 (GraphPad Software, San Diego, CA). Visualization was performed in GraphPad Prism 7 or R 3.5.2[41] using the ggplot2[42] and ggthemes packages.[43] Specific details of each analysis can be found in the respective figure legends.

3 | RESULTS

3.1 | Enrichment of primary mouse KCs and LSECs

Studies in rats and mice have indicated that KCs and LSECs are extremely vulnerable to the effects of ricin toxin.[20,24,44,45] To better understand the interaction of ricin toxin with these cell types and what role antibodies may play in protection, we sought to establish an ex vivo model with primary mouse KCs and LSECs. As depicted in Fig. 1, primary KCs and LSECs were isolated from the livers of Swiss Webster mice using a 2-step collagenase perfusion method. The 2 cell types were enriched using a combination of low-speed centrifugation, density gradient centrifugation, and Ab-conjugated magnetic microbeads.[46–49] For the magnetic separation, anti-F4/80 microbeads were used to positively select for mouse KCs. LSECs were collected in the flow-through (negative selection), as there are no known universal markers for these cell types to enable positive selection.[50–52] Although numerous studies have reported using anti-CD146 magnetic microbeads for LSECs selection, this strategy does not capture the $CD146^-$ cell subset.[48] For that reason, we relied on negative selection to enrich for both the $CD146^-$ and $CD146^+$ LSEC subsets.

To assess the relative enrichment of the 2 primary cell populations, the KC and LSEC pools were triple-stained with antibodies specific for F4/80, CD146, and CD45, and then subjected to flow cytometry.[53,54] The isolation and purification protocol yielded positively-selected KCs at 95.8 ± 0.608% enrichment, based on F4/80 and CD45 expression (Table 1 and Supplemental Fig. S1). The KCs were also positive for CD11b (data not shown). The average KC yield per mouse liver was $\sim 2 \times 10^6$, and cell viability was >90% (Table 1 and Supplemental Fig. S1E). The LSEC pool consisted of 2 subpopulations that varied in expression levels of CD45: $CD146^-/CD45^{hi}$ and $CD146^+/CD45^+$ (Table 1 and Supplemental Fig. S1). These 2 LSEC populations have been described previously in rats.[55] The $CD146^-$ subset is not hepatic stellate cells (HSCs) or vascular endothelial cells because those

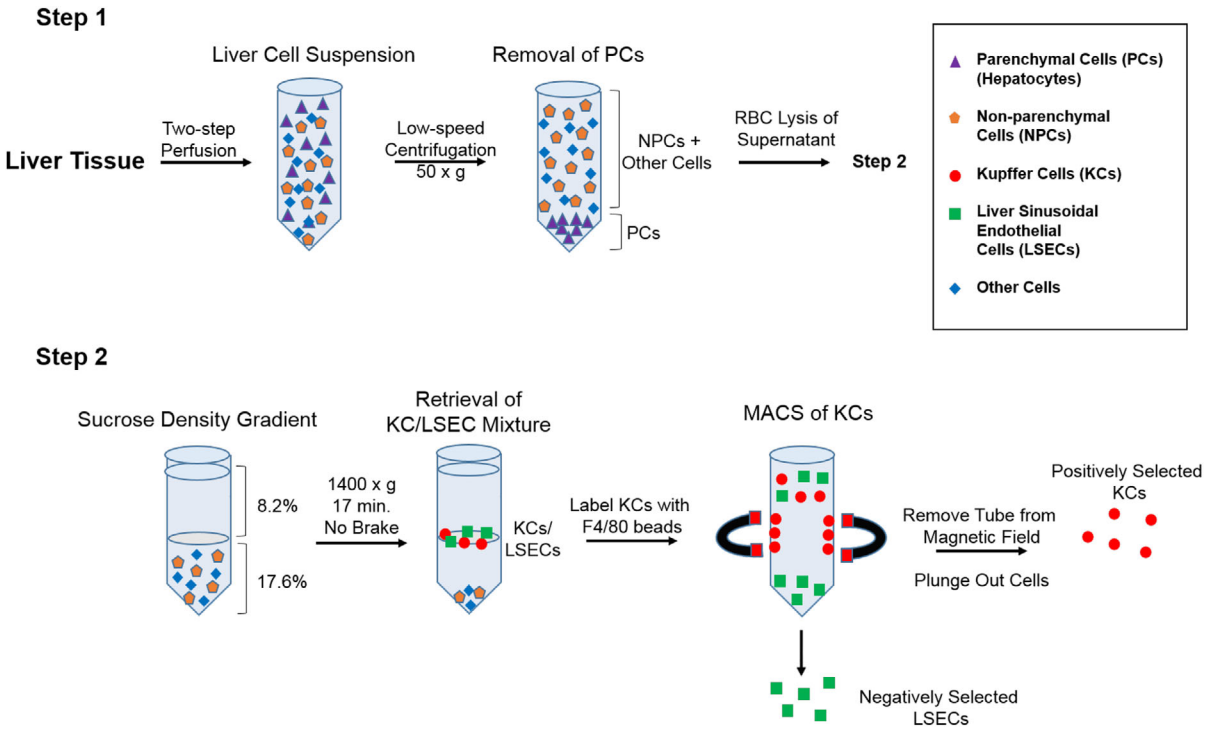

FIGURE 1 **Isolation and enrichment protocol for KCs and LSECs from mouse livers.** In Step 1, liver tissues were subjected to a retrograde 2-step perfusion followed by low speed centrifugation to remove hepatocytes. The RBCs were then lysed with ammonium chloride and the remaining cell mixture was subjected to sucrose density gradient centrifugation. In Step 2, the KC/LSECs populations partition was collected and mixed with anti-F4/80 antibody-coated magnetic beads. KCs were positively selected by magnetic separation, whereas LSECs were enriched in the flow through. Relative enrichment and viability of primary KCs and LSECs was determined by flow cytometry and phase contrast microscopy

TABLE 1 Enrichment and viability of mouse KCs and LSECs

	KCs[a]	LSECs[a]
Yield	$1.6–2.9 \times 10^6$	$7.07–11.0 \times 10^6$
% Purity[b]	95.8 ± 0.608	85.16 ± 1.76
% Viability (TB)	92.8 ± 2.58	90.42 ± 3.45
% Viability (PI)[c]	94.68 ± 2.55	91.79 ± 1.53

[a]Per mouse, based on positive KC or negative LSEC selection.
[b]Refer to Supplemental Fig. S1A–D for flow cytometry purity plots.
[c]Refer to Supplemental Fig. S1E and F for cell viability plots
TB, Trypan Blue; PI, propidium iodide.

TABLE 2 Sensitivity of LSECs, KCs, and J774E cells to ricin toxin and RTA[a]

	Ricin		RTA	
	EC_{50}	EC_{90}	EC_{50}	EC_{90}
LSEC	0.87	2.63	50.0	>400
KC	0.02	0.23	5.30	177
J774E	1.5	2.97	>400	>400

[a]EC_{50} and EC_{90} values in ng/ml after 18 h treatment (as described in the text).

2 cell types do not express CD45.[56,57] The LSEC pool also contained a fraction (~8%–10%) of contaminating KCs. The viability of LSECs was ~90% based on trypan blue (TB) and PI staining (Table 1 and Supplemental Fig. S1). Both the KC and LSEC populations adhered to collagen-coated microtiter plates and assumed morphologies consistent with KCs and LSECs (data not shown).[58,59]

We next examined the sensitivity of primary KCs and LSECs to ricin intoxication. J774E cells, a well-characterized mouse macrophage cell line reported to express the MR (CD206), were included as a control for these experiments.[60–62] Ricin cytotoxicity was initially evaluated across a range of KC and LSEC densities (1×10^4 to 1×10^5 cells total), as described in the section *Materials and Methods*. We ultimately chose 5×10^4 total cells as a working concentration as there was little variation in toxin sensitivity across the range of cell densities we tested (data not shown). Depending on the experiments, we performed cytotoxicity profiles with either a 2 h pulse with ricin or a prolonged (18 h) incubation period, followed by a series of wash steps to remove residual extracellular toxin before a 24 h incubation.

3.2 | Ex vivo sensitivity of KCs to ricin

KCs were remarkably sensitive to the effects of ricin toxin, as evidenced by EC_{50} values of 1.3 and 0.02 ng/ml in the 2 and 18 h exposure assays, respectively (Table 2 and Fig. 2). For J774E cells, EC_{50} values were 44 and 1.5 ng/ml for the 2 and 18 h exposures, respectively. Ricin toxin was reported to enter BDMCs by 2 distinct mechanisms: one mediated by RTB that is inhibited by lactose, and the other mediated by the MR that is inhibited by mannan.[6,8] By flow cytometry, we

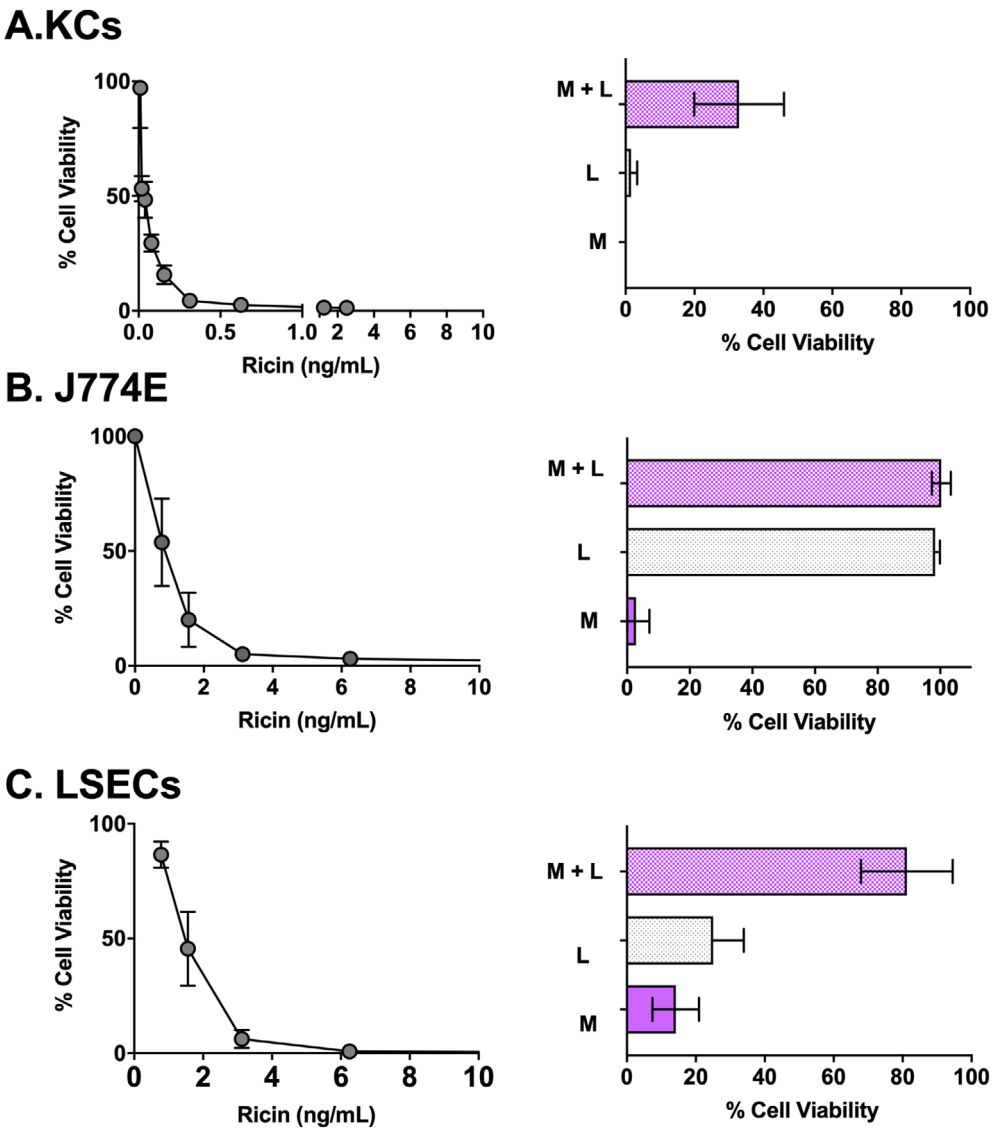

FIGURE 2 **Sensitivity of KCs, J774E cells, and LSECs to ricin toxin.** Left panels: Average cell viability of KCs (panel A), J774E cells (panel B), and LSECs (panel C) after an 18 h exposure to indicated concentrations of ricin toxin from 2 independent experiments. Right panels: Effects of coincubation of ricin with α-mannan (M; 1 mg/ml), lactose (L; 0.1 M), and the combination of α-mannan and lactose (M + L) on viability of the 3 different cell types. Each bar represents the average (with corresponding standard deviations) of 6 independent experiments

confirmed that the isolated mouse KC populations were positive for the MR (Supplemental Fig. S2).

To examine the contribution of these 2 pathways in ricin uptake, KCs were pulsed for 2 h with ricin in the presence of saturating amounts of exogenous lactose (0.1 M), α-mannan (1 mg/ml), or both lactose and α-mannan.[6,8] KC viability was assessed 24 h later. Neither lactose nor mannan alone abrogated the effect of ricin (Fig. 2). However, the combination of lactose and mannan afforded partial protection (~40% viability) against ricin-induced cell death, consistent with ricin internalization into KCs occurring via RTB and the MR. To examine the factors influencing ricin attachment to KCs, freshly isolated cells were incubated at 4°C and pulsed with FITC-labeled ricin in the absence or presence of a large excess of lactose, mannan, or the combination of lactose and mannan. After which the cells were analyzed by flow cytometry. Lactose inhibited ricin binding to KCs by ~90%, whereas mannan alone affected attachment by just ~10% (Supplemental Fig. S2). The combination of lactose and mannan did not significantly inhibit binding of ricin to KCs beyond lactose alone. These results indicate that the vast majority of ricin associates with KCs by virtue of RTB's Gal/GalNAc-specific lectin activity, whereas the MR accounts for just a fraction of ricin binding. However, despite the differences in binding, the 2 pathways apparently contribute equally to ricin uptake, as neither lactose nor mannan alone impacted ricin cytotoxicity on KCs. This apparent disconnect is explained by the fact that RTB-mediated uptake is inefficient, whereas the MR uptake is extremely efficient.[6,63] Thus, even small amounts of ricin bound to the MR can result in productive intoxication and cell death.

It should be pointed out that the mannan and lactose mixture only partially protected KCs from ricin, indicating the existence of a

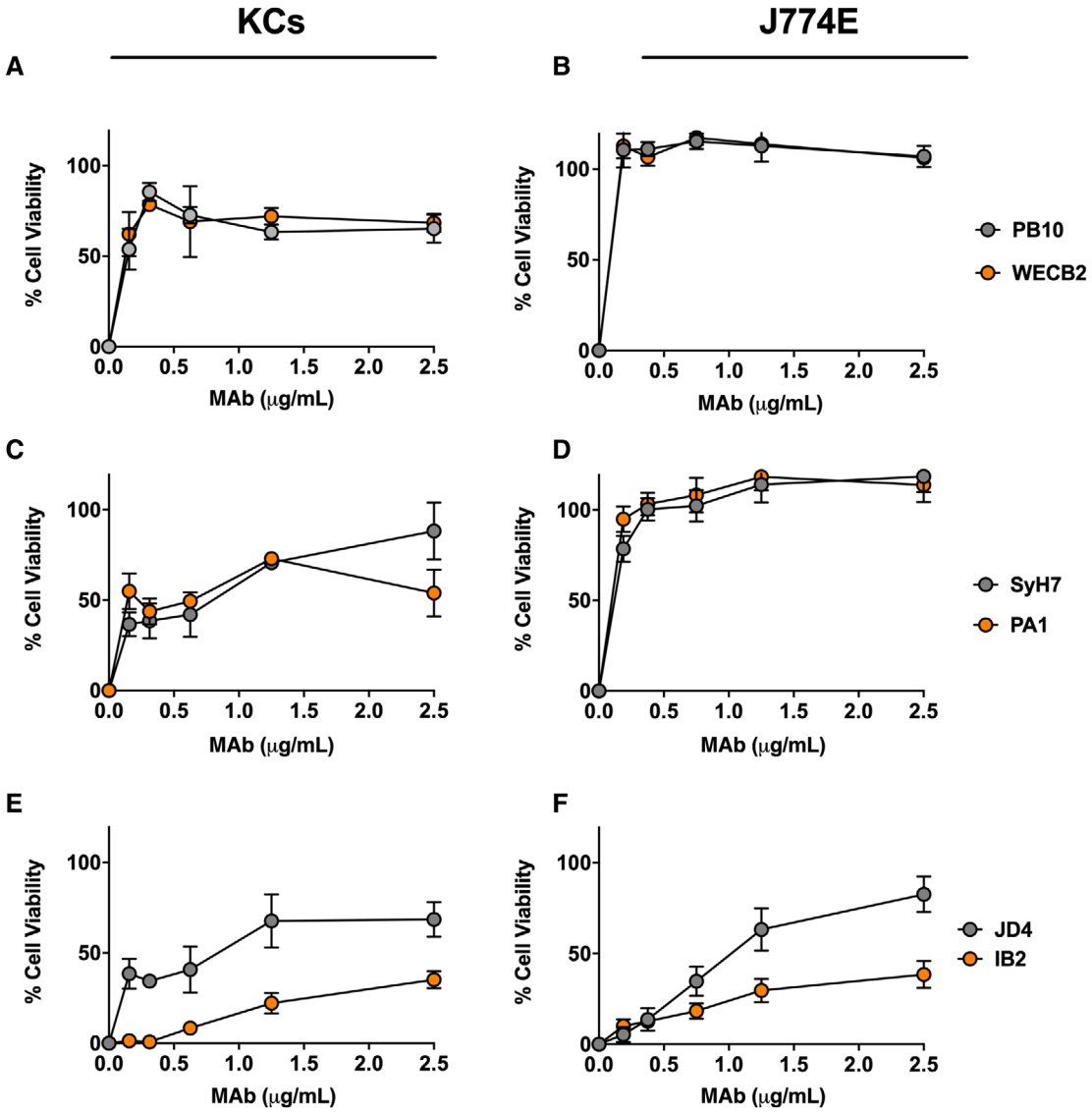

FIGURE 3 **Protection of KCs and J774E cells from ricin toxicity by individual anti-RTA MAbs.** Freshly isolated KCs (panels A, C, and E) or J774E cells (panels B, D, and F) were seeded into 96-well microtiter plates and then treated with ricin plus indicated amount of anti-RTA MAbs for 18 h. The cells were washed, and cell viability was assessed 24 h later. The MAbs are grouped based on their epitopes clusters on RTA: cluster I (A and B), cluster II (C and D) and Clusters III and IV (E and F). Each data point represents the average (with corresponding standard deviations) of 3 independent experiments

third uptake pathway in these cells. Although not investigated here, RTA-derived peptides containing the LDV sequence have been shown to trigger apoptosis of HUVECs via a process that is inhibited by fibronectin and likely integrin mediated.[64–66]

In the case of J774E cells, lactose alone completely inhibited ricin binding to cell surfaces and also protected cells from ricin intoxication (Fig. 2 and Supplemental Fig. S2). Mannan did not affect ricin attachment to J774E cells nor did it impact ricin's cytotoxic activity. Thus, ricin intoxication of J77E cells is solely dependent on RTB's lectin activity, even though the cells express the MR on their surface (Supplemental Fig. S2). MR expression and half-life has been reported to vary widely among different J774E clones, possibly explaining the failure of MR to promote ricin uptake here.[60]

3.3 | Capacity of anti-RTA and anti-RTB MAbs to protect KCs from ricin intoxication ex vivo

We next examined the capacity of ricin-specific MAbs to protect KCs against ricin toxicity ex vivo. We have previously described a collection anti-RTA and anti-RTB MAbs with a range of neutralizing activities (IC_{50}) on Vero cells.[29,31–35] The anti-RTA MAbs are directed against 4 spatially distinct epitope clusters (I–IV). PB10 and WECB2 recognize cluster I, SyH7 and PA1 recognize cluster II, and MAbs IB2 and JD4 bind clusters III and IV, respectively (Supplemental Table S1). The mechanisms of toxin neutralization may differ depending on epitope specificity.[67]

The 4 RTA-specific MAbs against epitope clusters I (PB10, WECB2) and II (SyH7, PA1) readily neutralized ricin on the J774E cells

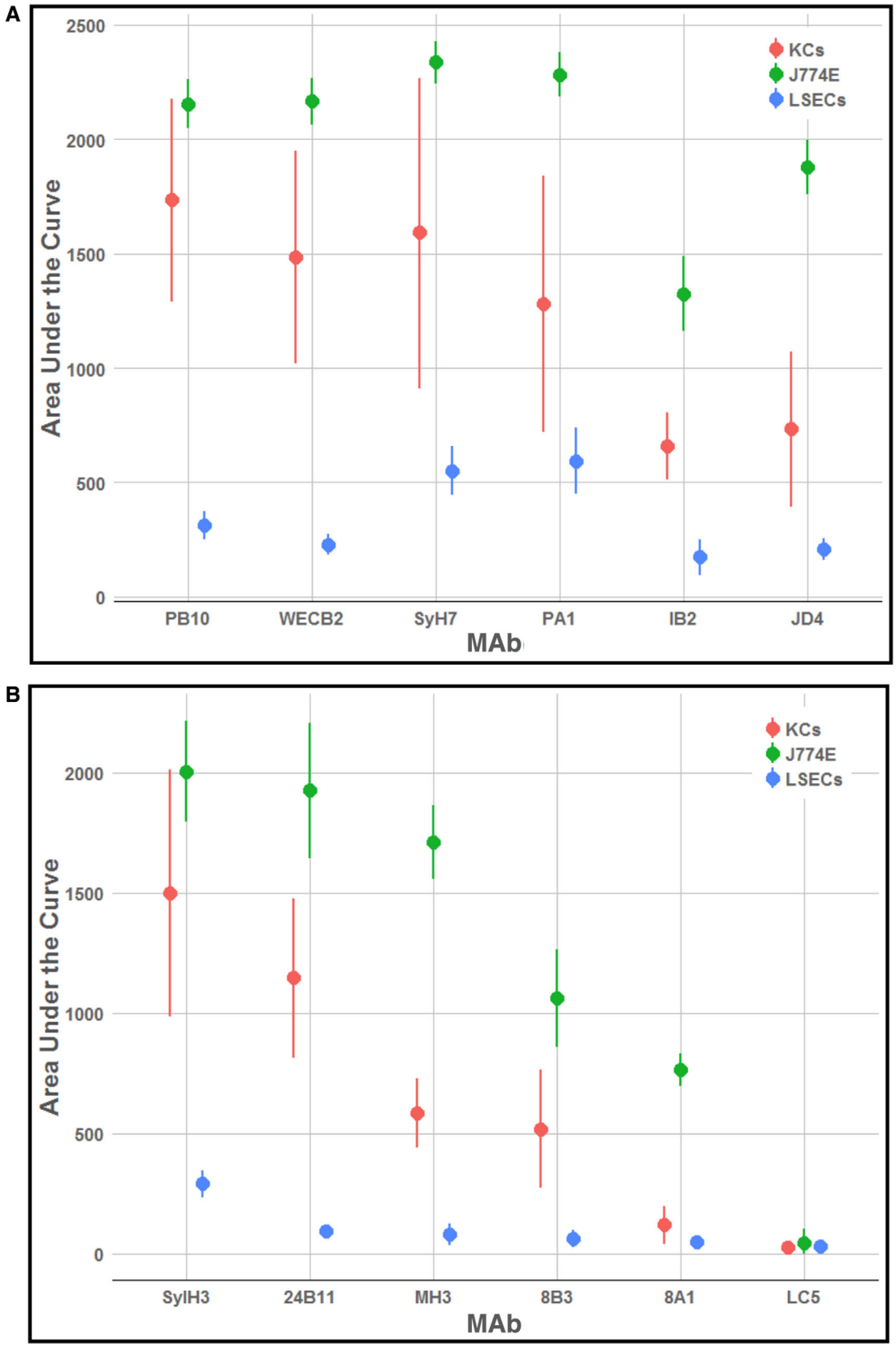

FIGURE 4 **Comparative analysis of anti-RTA and anti-RTB MAbs in protecting KCs, J774E, and LSECs from ricin toxin.** Area under the curve (AUC) analysis of ricin-toxin neutralizing activities of a collection of MAbs targeting (A) RTA and (B) RTB. Cytotoxicity assays were performed across a range of MAb concentrations (starting at 20 μg/ml), as described in the section *Materials and Methods*. AUC values and corresponding 95% confidence intervals were determined for each antibody from the results of ricin neutralization assays, with 4–13 biologic replicates per concentration

(IC_{50} < 0.2 μg/ml) (Fig. 3). The MAbs also protected KCs from ricin toxin (40%–80%), although much less effectively than in the J774E cell assay (Fig. 3). Moreover, PB10, WECB2, SyH7, and PA1 toxin-neutralizing activities plateaued at ~80% in the KCs, even at high MAb concentrations. IB2 and JD4 also afforded some degree of toxin-neutralizing activity on both J774E and KCs (Fig. 3). In addition, individual anti-RTB antibodies were able to partially protect KCs from ricin, but less effectively than in the J774E cytotoxicity assay (Supplemental Fig. S3). For comparison purposes, the overall toxin-neutralizing activity for each MAb tested in the KC and J774E assay was plotted as area under the curve (AUC) (Fig. 4). The plot illustrates the superior neutralizing activity of the MAbs in the J774E assay, as compared with the KC assay.

3.4 | Protecting KCs from ricin-induced killing in vivo

The results of the ex vivo studies prompted us to examine the degree to which individual anti-ricin MAbs are able to protect KCs in vivo. We chose PB10 (anti-RTA) and SylH3 (anti-RTB) for these studies as they represent 2 of our most potent classes of toxin-neutralizing MAbs.[18,33,34,68] Ricin was injected into mice by the i.p. or i.v. routes in absence or presence of PB10 or SylH3. It is known that injection of ricin into mice by the i.v. or i.p. routes results in toxin accumulation in liver.[69] The mice were euthanized 18 h later and KCs were isolated from livers as described above. In the absence of either PB10 or SylH3, the KC populations, defined by $F4/80^+$ staining, declined from ~23% to <2%, consistent with ricin's capacity to essentially ablate these cells from the liver (Fig. 5 and Supplemental Fig. S4). The loss of KCs in situ was confirmed by IHC analysis with F4/80 antibodies (Fig. 5). By comparison, coadministration of ricin with PB10 resulted in complete protection of KCs from toxin-induced death, as determined by flow cytometry and IHC. Identical results were obtained when ricin was coadministered by SylH3 and delivered to mice by i.v. injection (Supplemental Fig. S4). Thus, individual MAbs against RTA or RTB are able to protect KCs in vivo from the effects of ricin exposure, even though they afforded less than maximal activity ex vivo. From an intervention standpoint, a single MAb like PB10 or SylH3 would be considered appropriate to protect KCs against ricin.

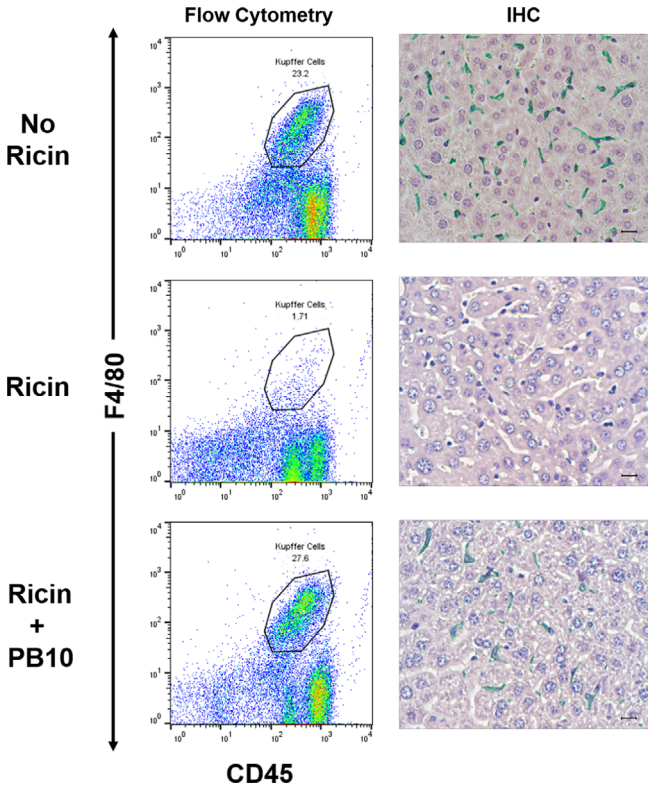

FIGURE 5 **PB10 protects KCs from the effects of ricin in vivo.** Groups of mice were challenged by i.p. injection with saline (top row), ricin toxin (middle row), or ricin toxin plus PB10 (bottom row). Eighteen hours later, the mice were euthanized, and liver tissues collected for KC isolation (left panels) or IHC (right panel). For flow cytometric analysis, KCs were immunostained for F4/80 (*y*-axis) and CD45 (*x*-axis), as described in the section *Materials and Methods*. The $CD45^+$ $F4/80^+$ KC populations are encircled, and the percentage of the total cell numbers are noted. For IHC (right panels), formalin-fixed tissue sections were stained with anti-F4/80 followed by HRP-based polymer and Vina Green chromogen, also as described in the section *Materials and Methods*. Note the complete absence of $F4/80^+$ cells in ricin treated mice, compared to near normal numbers of $F4/80^+$ cells in ricin plus PB10-treated animals

3.5 | Sensitivity and neutralizing activity of MAbs in LSEC assay

We next examined the sensitivity of LSECs to ricin. As shown in Table 2 and Fig. 2, ricin induced LSEC death in a dose-dependent manner, with an estimated EC_{50} of 4 ng/ml. Coadministration of ricin with either lactose (0.1 M) or α-mannan (1 mg/ml) afforded limited protection (20%–30%) against killing, whereas the combination of lactose and α-mannan resulted in ~80% viability. These results are consistent with ricin uptake into LSECs occurring via RTB- and MR-dependent pathways.[9] By flow cytometry, MR expression was detected on the $CD146^+$ LSEC population, but not the $CD146^-$ population (Supplemental Fig. S2).

Our collection of RTA-specific MAbs were evaluated for the ability to protect LSECs from the effects of ricin. Surprisingly, individual anti-RTA MAbs were largely, if not completely, ineffective at neutralizing ricin in the LSEC cytotoxicity assay (Figs. 4 and 6). For example, even molar excess amounts of PB10 afforded only 10% protection against ricin killing (Fig. 6). Two other MAbs, SyH7 and PA1, fared slightly better (~40% viability), but never achieved complete protection.

The failure of the individual MAbs to neutralize ricin in the LSEC cytotoxicity assay prompted us to test a combination of all 4 anti-RTA MAbs, effectively creating a quadrivalent cocktail targeting the 4 known neutralizing hotspots on RTA. The quadrivalent Ab mixture demonstrated extremely potent toxin-neutralizing activity in the LSEC cytotoxicity assay, with an IC_{50} of <0.2 μg/ml (Fig. 6). In an effort to ascribe the neutralizing activity to particular MAb combination, the 4 different MAbs were tested in all possible combinations (Supplemental Fig. S5). Certain pairs, namely PB10 and SyH7, afforded between 80% and 90% protection at high concentrations (>1 μg/ml), but no

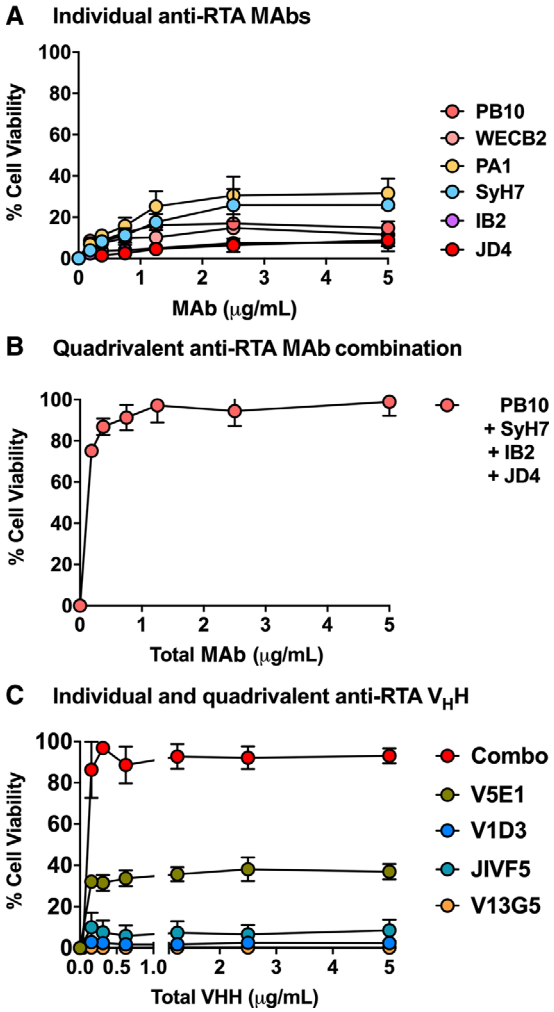

FIGURE 6 **Protection of LSECs by anti-RTA MAb cocktails.** LSECs were seeded in 96-well microtiter plates and then treated with ricin plus indicated concentrations of (panel A) individual anti-RTA MAbs, (panel B) an anti-RTA quadrivalent MAb cocktail, or (panel C) individual and combinations of anti-RTA V_HHs. Cell viability was normalized to LSECs treated with vehicle (saline), as described in the section *Materials and Methods*. Each data point represents the average (with corresponding standard deviations) of 3 independent experiments

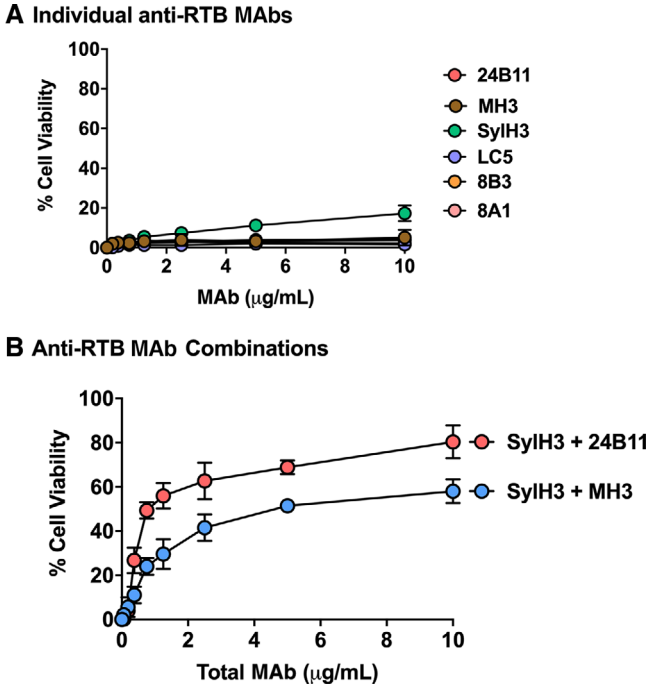

FIGURE 7 **Protection of LSECs by individual and pairs of anti-RTB MAbs.** LSECs were seeded into 96-well microtiter plates and then treated with ricin with individual MAbs (panel A) or pairs of RTB-specific MAbs (panel B) at indicated total concentrations, as described in the section *Materials and Methods*. Each data point represents the average (with corresponding standard deviations) of 3 independent experiments

2 or 3 MAb combination achieved the potency observed with the quadrivalent cocktail.

To further examine the combinatorial effects of antibodies on ricin toxin neutralizing activity in the LSEC cytotoxicity assay, we turned to a collection of alpaca-derived single domain antibodies (V_HHs).[39,70] V_HHs differ from conventional IgG MAbs in that they are monovalent and are devoid of Fc elements, thereby eliminating any contribution of aggregation and FcR involvement in the cytotoxicity assay. V_HHs targeting RTA's 4 neutralizing hotspots were tested individually and in combination. Although only 1 of the 4 individual V_HHs had notable toxin-neutralizing activity on its own, the quadrivalent mixture proved nearly as potent at inactivating ricin as the 4 MAb cocktail (Fig. 6). Thus, co-occupancy of key neutralizing epitopes on RTA rather than agglutination or FcR-mediated uptake is likely responsible for the protection of LSECs from the effects of ricin.

A similar pattern emerged when we tested a collection of anti-RTB mouse IgG MAbs and alpaca V_HHs in the LSEC cytotoxicity assay (Supplemental Table S1 and Fig. 7). Neither the individual anti-RTB MAbs (Fig. 7A) nor the individual V_HHs (data not shown) demonstrated a capacity to neutralize ricin in the LSEC assay. Mixtures of SylH3 combined with MH3 or 24B11 had only moderate toxin-neutralizing activity (50%–75%) (Fig. 7B).

3.6 | Pairs of anti-RTA/anti-RTB MAbs protect LSECs from ricin intoxication

The next obvious line of investigation was to examine toxin-neutralizing activity of pairs of anti-RTA and anti-RTB MAbs. We generated 4 different anti-RTA and anti-RTB MAb combinations using PB10, SyH7, SylH3, and 24B11. All 4 anti-RTA/anti-RTB cocktails demonstrated remarkably potent toxin-neutralizing activity, as evidenced by IC_{50} values of <0.2 μg/ml (Fig. 8A). In fact, the toxin-neutralizing profiles were essentially superimposable, indicating that equal potency was achieved irrespective of the different epitopes being targeted on RTA (i.e., cluster I or II) and RTB (i.e., domain 1 or 2).

We also tested the potency of 2 different pairs of anti-RTA/anti-RTB V_HHs single chain antibodies. Two different V_HH pairs demonstrated potent toxin-neutralizing activities, although not to the extent observed with the MAbs (Fig. 8B). Nonetheless, the activity associated with the V_HH pairs was much greater than additive effects,

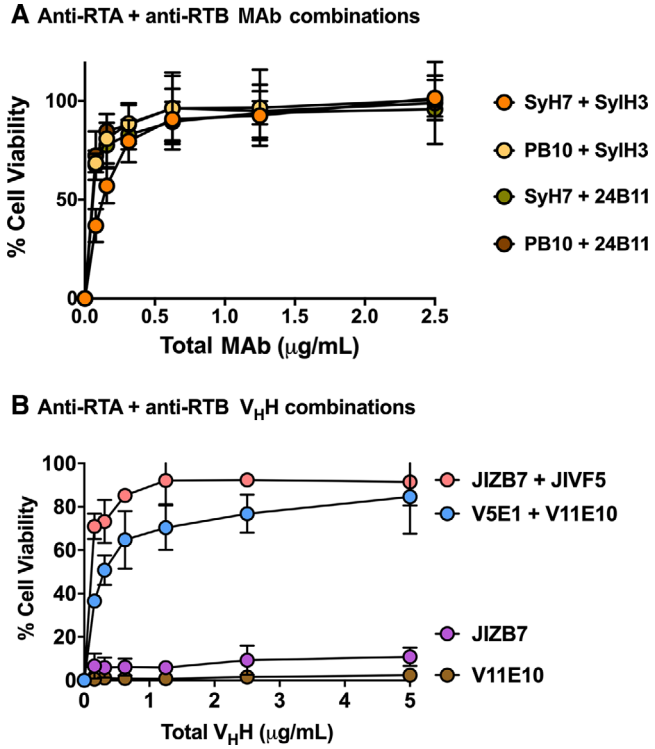

FIGURE 8 Protection of LSECs by MAb and V_HH cocktails. LSECs were seeded into 96-well microtiter plates and then challenged ricin toxin incubated with pairs of anti-RTA (PB10, SyH7) and anti-RTB (SylH3, 24B11) MAbs (panel A) and V_HHs (panel B). V11E10 is against RTA, and JIZB7 against RTB. Each data point represents the average (with corresponding standard deviations) of 3 independent experiments

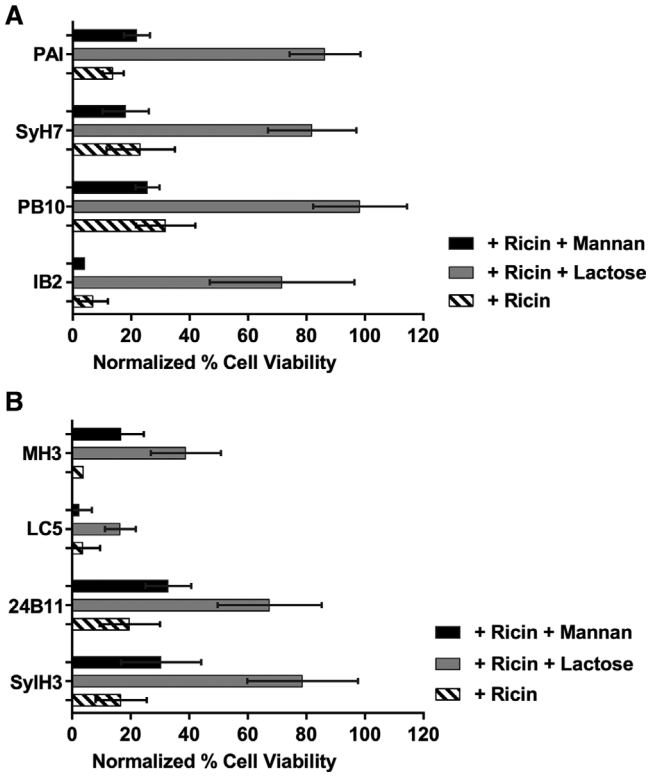

FIGURE 9 Anti-ricin MAbs function via the mannan-dependent uptake pathway in LSECs. Freshly isolated LSECs were seeded in 96-well microtiter plates and pulsed for 2 h with ricin plus indicated anti-RTA (panel A) or anti-RTB (panel B) MAbs, in the presence of α-mannan (1 mg/ml) or lactose (0.1 M). Cell viability was normalized to LSECs that had not been treated with ricin toxin. In all cases, the addition of lactose resulted in a significant increase in cell viability, as compared with the control (ricin only). Mannan addition impacted cell viability in only 1 instance (MH3). Kruskal–Wallis with Tukey's multiple comparisons test (GraphPad 7) was applied to account for non-normal distribution of data

indicating that targeting both of ricin's subunits simultaneously results in synergistic activity and therefore an effective means to protect LSECs from ricin.

3.7 | Anti-RTA and anti-RTB MAbs neutralize ricin via the mannose-dependent uptake pathway in LSECs

We hypothesized that the observed synergy between anti-RTA and anti-RTB MAbs in the LSECs cytotoxicity assay might be explained by the MAbs acting on different ricin uptake pathways. Based on the literature, we postulated that anti-RTB MAbs block the lactose-dependent uptake pathway, whereas anti-RTA MAbs interfere with the mannan-dependent pathway.[29,67,71] To test this hypothesis, individual MAbs were mixed with lactose (to block RTB-mediated uptake) or mannan (to block the MR and other CTL uptake) and then tested them for the ability to protect LSECs from ricin challenge.

We found that the neutralizing activity of the anti-RTA MAbs was significantly enhanced by the addition of lactose, but not mannan (Fig. 9). For example, LSEC viability in the presence of ricin and PB10 was ~30%, whereas the further addition of lactose resulted in >90% viability. The same was observed for MAbs SyH7 and PA1 (directed against epitope cluster II) and IB2 (against epitope cluster III). Overall, these results are consistent with anti-RTA MAbs blocking ricin uptake via the MR (or another mannose-dependent CTL) in the LSEC cytotoxicity assay, not the lactose uptake pathway.

Unexpectedly, the toxin-neutralizing activity of the anti-RTB MAbs was also enhanced by lactose. For example, the addition of lactose enhanced 24B11 and SylH3's activities from ~20% viability to ~80% viability. The addition of mannan enhanced neutralizing activity to just 30% viability (Fig. 9). MH3's toxin-neutralizing activity was also enhanced by lactose and mannan, although total LSEC viability never exceeded 50%. These results suggest that anti-RTB MAbs may also interfere with ricin uptake via the MR pathway, not the lactose-dependent uptake pathway as we had postulated.

The fact that SylH3 and PB10 plus lactose are much more effective than saturating amounts of mannan plus lactose at protecting LSECs from ricin intoxication indicates that the MAbs have "effector functions" not mimicked by mannan. We postulate that the most plausible explanation is simply binding affinity. For example, PB10 and SylH3 each bind to ricin with subnanomolar affinities and would be expected to stay associated with ricin following endocytosis, whereas mannan has only micromolar affinity for the MR and would be expected to serve

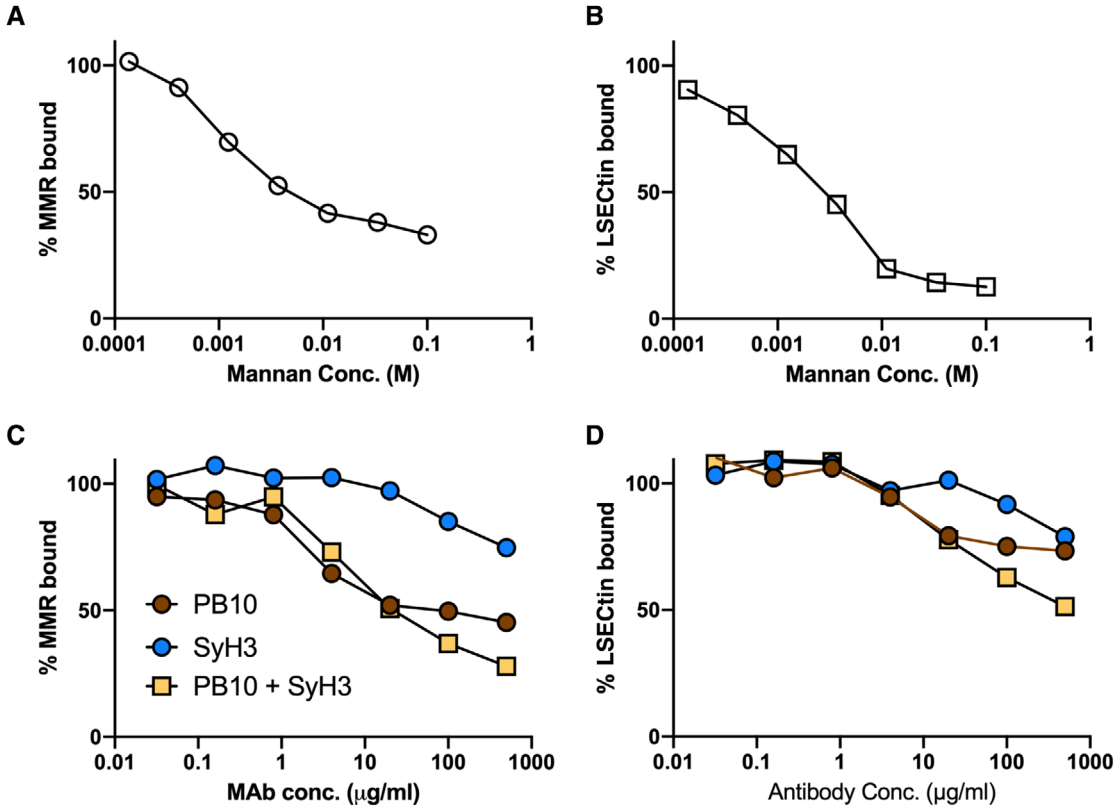

FIGURE 10 **Effect of MAbs on the interaction between ricin and the MR and LSECtin**. Immulon microtiter plates were coated with ricin (1 μg/ml) and then probed with recombinant mouse MR or LSECtin, as described in the section *Materials and Methods*, in the presence of increasing amounts of mannan (panels A and B) or 5-fold serial dilutions of MAbs (panels C and D). Shown are the averages of representative experiments with 3 technical replicates

as a relatively weak competitive inhibitor, even at saturating doses. However, the story could be more complicated if the ricin–MAb complexes are delivered into the cytosol where actors like TRIM-21 are able to promote the clearance of IgG-based immune complexes.[72]

3.8 | Interaction of ricin with the MR and LSECtin

To examine the possibility that anti-RTA and anti-RTB MAbs interfere with toxin–MR interactions, we established a solid phase binding assay in which immobilized ricin toxin was probed with recombinant mouse MR. The interaction of the MR with immobilized ricin was inhibited by mannan in a dose-dependent manner (Fig. 10). At high concentrations, PB10 and the PB10/SylH3 combination partially inhibited (50%–60% reduction) the binding of the MR to ricin. SylH3 also affected the MR-ricin interaction but to a lesser extent, although it is unclear whether these reductions in binding account for the observed effects of the MAbs on toxin-neutralizing activity.

We also established a binding assay between ricin and LSECtin (CLEC4G), another CTL enriched in the liver that recognizes GlcNAcMan residues like those on RTA and RTB.[73] LSECtin recognized immobilized ricin in a mannose-dependent manner, although neither PB10 nor SyH3 were particularly effective at blocking this interaction (Fig. 10). Collectively, these results suggest that PB10 and SylH3 protect LSECs from ricin toxin by a mechanism other than interfering with the initial recognition between ricin and the MR or another CTL receptor such as LSECtin.

3.9 | A candidate ricin toxin subunit vaccine elicits antibodies that protect KCs and LSECs from ricin

RiVax is a recombinant RTA subunit vaccine that has been shown to elicit immunity to ricin in mice and nonhuman primates.[74,75] It is also safe in humans when administered intramuscularly.[76] We therefore wished to examine whether anti-RiVax antisera is able to protect KCs and LSECs ex vivo. Ricin was incubated with serial dilutions of antisera from RiVax vaccinated mice and then applied to KCs and LSECs. We found that the anti-serum had similar IC_{50} titers (e.g., 1:2500) for both KCs and LSECs, consistent with roughly equal degrees of protection (Supplemental Fig. S6). This result may explain in part the relative efficacy of RiVax as a vaccine against ricin intoxication.

4 | DISCUSSION

The liver plays an essential role in detoxification and clearance of xenobiotics from circulation.[25,77] Nonparenchymal cells also function in immune surveillance and uptake of SIC.[28,78,79] In this report, we investigated the capacity of anti-RTA and anti-RTB MAbs, individually

and in combination, to protect primary mouse KCs and LSECs from ricin toxin-induced death. This study was motivated by the fact that KCs and LSECs are notoriously sensitive to the effects of ricin, a point recognized decades ago when RTA was first being explored as an immunotoxin.[7,45,80–83] Indeed, we found that freshly isolated mouse KCs were 10–40 times more sensitive to ricin than standard mouse cell lines like J774E cells. Nonetheless, individual MAbs against RTA or RTB were able to protect KCs ex vivo with efficiencies similar to J774E cells. In addition, 2 MAbs, PB10 and SyH3, were each able to protect KCs from ricin-induced apoptosis in vivo. Thus, despite their remarkable sensitivity to ricin toxin, KCs are readily protected from toxin-induced death by anti-RTA and anti-RTB MAbs.

LSECs were another story. We found that individual anti-RTA and anti-RTB MAbs had virtually no capacity to protect LSECs from ricin intoxication. For example, even PB10, which has been shown to be able to rescue Rhesus macaques from lethal dose ricin exposure by aerosol, afforded less than 20% protection in the LSEC killing assay. This shortcoming was overcome when PB10 was combined with other MAbs. The most effective combination was a 2-part cocktail targeting RTA and RTB (i.e., PB10 + SyH3), although other pairs and oligoclonal mixtures were equally functional. Combinations of V_HHs, which are monovalent and lack Fc elements, also had neutralizing activity, demonstrating that neither ricin crosslinking (aggregation) nor FcR engagement is necessary to protect LSECs from ricin intoxication.

When considering possible mechanisms by which MAbs protect KCs and LSECs, it is important to keep in mind that ricin uptake by these 2 cell types occurs by at least 2 distinct pathways: one inhibited by exogenous lactose ("lactose-sensitive") and the other by exogenous mannose or mannan ("mannose-sensitive"). The lactose-dependent endocytic pathway, which has been studied in great detail, is mediated by RTB's affinity for terminal Gal/GalNAc residues on cell surface glycoproteins and glycolipids.[63] Following endocytosis, ricin holotoxin is trafficked retrograde to the TGN and the ER, where RTA is liberated from RTB and translocated into the cytoplasm.[84] This uptake pathway is inefficient, however, as only a small fraction (1%–10%) of the total amount of ricin bound to any given cell surface actually results in delivery of RTA into the cytoplasm.[84,85] Moreover, ricin is easily derailed during retrograde transport, particularly if the toxin is aggregated or complexed with another protein.[86] All things considered, perhaps it is not surprising that ricin–MAb complexes are recycled or inefficiently routed to the TGN.[67,71,87]

The mannose-sensitive uptake pathway exploited by ricin to intoxicate liver cells is much less well understood. Although uptake has historically been attributed to the MR, this assumption is inconsistent with demonstration that MR knock-out mice are significantly more susceptible (not more resistant) to toxin-induced death than age-matched controls.[6,8–10,88] Moreover, LSECs are sensitive to ricin toxin even though the MR is only expressed on the CD146+/CD45+ LSEC subset (~18% of total population) and not on the CD146-/CD45+ subset. Therefore, it is plausible that mannose-sensitive uptake of ricin is mediated by a second CTL. One candidate is LSECtin, a single domain CTL with homology to DC-SIGN and DC-SIGNR expressed exclusively in the liver.[89] LSECtin serves as a receptor for Ebola virus, SARS coronavirus, and Japanese encephalitis virus.[73,90] We found that recombinant LSECtin recognized ricin toxin in a solid phase binding assay and that the interaction was inhibited by mannan. Assessing the contribution of LSECtin in promoting ricin intoxication of LSECs in vivo awaits testing in LSECtin knockout mice.[91]

Nevertheless, it remains unclear how ricin and ricin-IC evade degradation following uptake by LSECs. A cardinal feature of LSECs is their extraordinary capacity to degrade endocytosed materials, including SIC.[26,27,50,92,93] Scavenging receptors like the MR, for example, release cargo within acidified endosomes before being recycled back to the cell surface.[94,95] That cargo is then destined for degradation via the lysosome or proteolytically processed and loaded onto major histocompatibility complexes. How ricin evades these fates following uptake by the MR or another CTL is unknown. There is evidence that ricin passes through an acidic compartment following uptake via the mannose-sensitive pathway, but ricin has no known mechanism to breach the endocytic membrane.[6]

Similarly, ricin–MAb complexes such as those generated in this study would be expected to be taken up by LSECs by way of FcγRIIb2.[28,79,96,97] FcγRIIb2 is an inhibitory Fc-receptor primarily expressed on LSECs and secondarily on KCs and is the largest contributor to clearance of SICs from circulation. Although FcγRIIB would not be able to internalize one-to-one toxin–Ab complexes (e.g., PB10-ricin), it would be predicted to engage with ricin decorated by 2 or more MAbs (e.g., PB10 + SyH3) and route them for degradation. Whether or not FcγRIIB plays a role in clearance of ricin immune complexes in vivo remains to be determined.

Our study adds to the growing list of examples in which MAb cocktails display synergistic neutralizing activity well beyond what is achieved with single MAbs alone.[98–101] In the case of botulinum neurotoxin (BoNT), for example, there is synergy with 2- and 3-component MAb cocktails that was attributed to either conformational changes induced by 1 Ab that enhanced secondary Ab recognition and/or toxin aggregation/multimerization.[102–104] In the case staphylococcus enterotoxin B (SEB), the combination of a MAb (20B1) that occludes the T-cell receptor binding site with MAbs of lesser (6D3,14G8) neutralizing activity enhanced Fc-mediated clearance of SEB in a mouse model. Similarly, combinations of non-neutralizing MAbs have been shown to neutralize Ebola and Marburg virus in animal models.[100,101] In a companion study, we demonstrated that the 2-part cocktail consisting of PB10 + SyH3 is far superior at protecting AMs and tissue resident macrophages from ricin-induced death in vivo, as compared with either of the MAbs individually (Rong et al., *manuscript submitted*). AMs are hypersensitive to the effects of ricin, possibly due to high levels of MR expression.[105] The success of PB10 + SylH3 in that study and the current study has prompted us to generate a humanized version of SyH3 with the goal of testing it in combination with humanized PB10 in the Rhesus macaque model.[17]

One limitation of our study is that we restricted our examination of the liver to LSECs and KCs, essentially ignoring other effects that ricin and ricin-IC may have on hepatic cellularity, inflammation, and physiology. For example, Roche and colleagues demonstrated in mice that hepatic inflammation and pathology following ricin exposure

includes an influx of neutrophils, chemokine expression (e.g., MCP-1), fibrin deposition, red blood cell congestion of the hepatic parenchyma and glycogen depletion.[106] These are obvious metrics that could be examined in the context of the MAbs and MAb cocktails like PB10 and SylH3 when administered concurrently or at timepoints after ricin challenge. Roche and colleagues did demonstrate a marked reduction in hepatic damage with the addition of anti-RTA MAbs and MAbs cocktails.

AUTHORSHIP

B.M., F.J.T.V., and J.D. performed the experiments; B.M., F.J.T.V., J.D., D.E., and N.J.M. analyzed results and prepared figures; B.M. and N.J.M. wrote the manuscript; N.J.M. was responsible for project administration and funding acquisition.

ACKNOWLEDGMENTS

We are grateful Dr. Renjie Song (Wadsworth Center Immunology Core Facility) for his assistance with flow cytometry. We extend a special thanks to Helen Johnson of the Wadsworth Center's Histopathology Core facility for preparation of tissue sections. We thank Dr. David Vance for providing V_HHs. We are grateful to Dr. Yinghui Rong for her scientific input and technical advice throughout the course of the study. We acknowledge Beth Cavosie for administrative assistance. Research reported in this work was supported by Contract No. HHSN272201400021C from the National Institutes of Allergy and Infectious Diseases, National Institutes of Health. The content is solely the responsibility of the authors and does not necessarily represent the official views of the National Institutes of Health. The funders had no role in study design, data collection and analysis, decision to publish, or preparation of the manuscript.

DISCLOSURES

The authors declare no conflicts of interest.

ORCID

Dylan J. Ehrbar https://orcid.org/0000-0001-7872-3338
Nicholas J. Mantis https://orcid.org/0000-0002-5083-8640

REFERENCES

1. Audi J, Belson M, Patel M, Schier J, Osterloh J. Ricin poisoning: a comprehensive review. *JAMA*. 2005;294:2342-2351.
2. Cieslak TJ, Kortepeter MG, Wojtyk RJ, et al. Beyond the dirty dozen: a proposed methodology for assessing future bioweapon threats. *Mil Med*. 2018;183:e59-e65.
3. Endo Y, Mitsui K, Motizuki M, Tsurugi K. The mechanism of action of ricin and related toxic lectins on eukaryotic ribosomes. The site and the characteristics of the modification in 28 S ribosomal RNA caused by the toxins. *J Biol Chem*. 1987;262:5908-5912.
4. Endo Y, Tsurugi K. RNA N-glycosidase activity of ricin A-chain. Mechanism of action of the toxic lectin ricin on eukaryotic ribosomes. *J Biol Chem*. 1987;262:8128-8130.
5. Tesh VL. The induction of apoptosis by Shiga toxins and ricin. *Curr Top Microbiol Immunol*. 2012;357:137-178.
6. Simmons BM, Stahl PD, Russell JH. Mannose receptor-mediated uptake of ricin toxin and ricin A chain by macrophages. Multiple intracellular pathways for a chain translocation. *J Biol Chem*. 1986;261:7912-7920.
7. Bourrie BJ, Casellas P, Blythman HE, Jansen FK. Study of the plasma clearance of antibody–ricin-A-chain immunotoxins. Evidence for specific recognition sites on the A chain that mediate rapid clearance of the immunotoxin. *Eur J Biochem*. 1986;155:1-10.
8. Magnusson S, Berg T. Endocytosis of ricin by rat liver cells in vivo and in vitro is mainly mediated by mannose receptors on sinusoidal endothelial cells. *Biochem J*. 1993;291(Pt 3):749-755.
9. Magnusson S, Berg T, Turpin E, Frenoy JP. Interactions of ricin with sinusoidal endothelial rat liver cells. Different involvement of two distinct carbohydrate-specific mechanisms in surface binding and internalization. *Biochem J*. 1991;277(Pt 3):855-861.
10. Magnusson S, Kjeken R, Berg T. Characterization of two distinct pathways of endocytosis of ricin by rat liver endothelial cells. *Exp Cell Res*. 1993;205:118-125.
11. Newton DL, Wales R, Richardson PT, et al. Cell surface and intracellular functions for ricin galactose binding. *J Biol Chem*. 1992;267:11917-11922.
12. Rutenber E, Katzin BJ, Ernst S, et al. Crystallographic refinement of ricin to 2.5 A. *Proteins*. 1991;10:240-250.
13. Youle RJ, Murray GJ. Studies on the galactose-binding site of ricin and the hybrid toxin Man6P-ricin. *Cell*. 1981;23:551-559.
14. Hadebe S, Brombacher F, Brown GD. C-type lectin receptors in asthma. *Front Immunol*. 2018;9:733.
15. Gal Y, Mazor O, Falach R, Sapoznikov A, Kronman C, Sabo T. Treatments for pulmonary ricin intoxication: current aspects and future prospects. *Toxins (Basel)*. 2017;9.
16. Rosenfeld R, Alcalay R, Mechaly A, et al. Improved antibody-based ricin neutralization by affinity maturation is correlated with slower off-rate values. *Protein Eng Des Sel*. 2017;30:611-617.
17. Roy CJ, Ehrbar DJ, Bohorova N, et al. Rescue of rhesus macaques from the lethality of aerosolized ricin toxin. *JCI Insight*. 2019;4.
18. Van Slyke G, Sully EK, Bohorova N, et al. Humanized monoclonal antibody that passively protects mice against systemic and intranasal ricin toxin challenge. *Clin Vaccine Immunol*. 2016;23:795-799.
19. Bhaskaran M, Didier PJ, Sivasubramani SK, Doyle LA, Holley J, Roy CJ. Pathology of lethal and sublethal doses of aerosolized ricin in rhesus macaques. *Toxicol Pathol*. 2014;42:573-581.
20. Bingen A, Creppy EE, Gut JP, Dirheimer G, Kirn A. The Kupffer cell is the first target in ricin-induced hepatitis. *J Submicrosc Cytol*. 1987;19:247-256.
21. Frenoy JP, Turpin E, Janicot M, Gehin-Fouque F, Desbuquois B. Uptake of injected 125I-ricin by rat liver in vivo. Subcellular distribution and characterization of the internalized ligand. *Biochem J*. 1992;284(Pt 1):249-257.
22. Skilleter DN, Foxwell BM. Selective uptake of ricin A-chain by hepatic non-parenchymal cells in vitro. Importance of mannose oligosaccharides in the toxin. *FEBS Lett*. 1986;196:344-348.
23. Worrell NR, Skilleter DN, Cumber AJ, Price RJ. Mannose receptor dependent uptake of a ricin A chain–antibody conjugate by rat liver non-parenchymal cells. *Biochem Biophys Res Commun*. 1986;137:892-896.
24. Zenilman ME, Fiani M, Stahl PD, Brunt EM, Flye MW. Selective depletion of Kupffer cells in mice by intact ricin. *Transplantation*. 1989;47:200-203.
25. Lee SJ, Evers S, Roeder D, et al. Mannose receptor-mediated regulation of serum glycoprotein homeostasis. *Science*. 2002;295:1898-1901.
26. Maynard Y, Baenziger JU. Oligosaccharide specific endocytosis by isolated rat hepatic reticuloendothelial cells. *J Biol Chem*. 1981;256:8063-8068.

27. Anderson CL. The liver sinusoidal endothelium reappears after being eclipsed by the Kupffer cell: a 20th century biological delusion corrected. *J Leukoc Biol*. 2015;98:875-876.
28. Ganesan LP, Kim J, Wu Y, et al. FcgammaRIIb on liver sinusoidal endothelium clears small immune complexes. *J Immunol*. 2012;189:4981-4988.
29. Yermakova A, Mantis NJ. Protective immunity to ricin toxin conferred by antibodies against the toxin's binding subunit (RTB). *Vaccine*. 2011;29:7925-7935.
30. Leshin J, Danielsen M, Credle JJ, Weeks A, O'Connell KP, Dretchen K. Characterization of ricin toxin family members from Ricinus communis. *Toxicon*. 2010;55:658-661.
31. Toth RTI, Angalakurthi SK, Van Slyke G, et al. High-definition mapping of four spatially distinct neutralizing epitope clusters on rivax, a candidate ricin toxin subunit vaccine. *Clin Vaccine Immunol*. 2017;24.
32. O'Hara JM, Kasten-Jolly JC, Reynolds CE, Mantis NJ. Localization of non-linear neutralizing B cell epitopes on ricin toxin's enzymatic subunit (RTA). *Immunol Lett*. 2014;158:7-13.
33. O'Hara JM, Neal LM, McCarthy EA, Kasten-Jolly JA, Brey RN, 3rd, Mantis NJ. Folding domains within the ricin toxin A subunit as targets of protective antibodies. *Vaccine*. 2010;28:7035-7046.
34. Rong Y, Van Slyke G, Vance DJ, Westfall J, Ehrbar D, Mantis NJ. Spatial location of neutralizing and non-neutralizing B cell epitopes on domain 1 of ricin toxin's binding subunit. *PLoS One*. 2017;12:e0180999.
35. Yermakova A, Vance DJ, Mantis NJ. Sub-domains of Ricin's B subunit as targets of toxin neutralizing and non-neutralizing monoclonal antibodies. *PLoS One*. 2012;7:e44317.
36. Rudolph MJ, Vance DJ, Cassidy MS, Rong Y, Mantis NJ. Structural analysis of single domain antibodies bound to a second neutralizing hot spot on ricin toxin's enzymatic subunit. *J Biol Chem*. 2017;292:872-883.
37. Rudolph MJ, Vance DJ, Cassidy MS, Rong Y, Shoemaker CB, Mantis NJ. Structural analysis of nested neutralizing and non-neutralizing B cell epitopes on ricin toxin's enzymatic subunit. *Proteins*. 2016;84:1162-1172.
38. Rudolph MJ, Vance DJ, Cheung J, et al. Crystal structures of ricin toxin's enzymatic subunit (RTA) in complex with neutralizing and non-neutralizing single-chain antibodies. *J Mol Biol*. 2014;426:3057-3068.
39. Vance DJ, Tremblay JM, Rong Y, et al. High-resolution epitope positioning of a large collection of neutralizing and nonneutralizing single-domain antibodies on the enzymatic and binding subunits of ricin toxin. *Clin Vaccine Immunol*. 2017;24.
40. Vance DJ, Greene CJ, Rong Y, Mandell LM, Connell TD, Mantis NJ. Comparative adjuvant effects of type II heat-labile enterotoxins in combination with two different candidate ricin toxin vaccine antigens. *Clin Vaccine Immunol*. 2015;22:1285-1293.
41. R_Core_Team. *R: A Language and Environment for Statistical Computing*. Vienna, Austria: R Foundation for Statistical Computing; 2014.
42. Wickham H. *ggplot2: Elegant Graphics for Data Analysis*. New York: Springer-Verlag New York; 2009.
43. Arnold JB, 2019 ggthemes: Extra Themes, Scales and Geoms for 'ggplot2'.
44. Derenzini M, Bonetti E, Marionozzi V, Stirpe F. Toxic effects of ricin: studies on the pathogenesis of liver lesions. *Virchows Arch B Cell Pathol*. 1976;20:15-28.
45. Zenilman ME, Fiani M, Stahl P, Brunt E, Flye MW. Use of ricin A-chain to selectively deplete Kupffer cells. *J Surg Res*. 1988;45:82-89.
46. Liu J, Huang X, Werner M, Broering R, Yang D, Lu M. Advanced method for isolation of mouse hepatocytes, liver sinusoidal endothelial cells, and Kupffer cells. In: Guo H, Cuconati A, eds. *Hepatitis B Virus: Methods and Protocols*. New York, NY: Springer New York; 2017.
47. Liu W, Hou Y, Chen H, et al. Sample preparation method for isolation of single-cell types from mouse liver for proteomic studies. *Proteomics*. 2011;11:3556-3564.
48. Meyer J, Gonelle-Gispert C, Morel P, Buhler L. Methods for isolation and purification of murine liver sinusoidal endothelial cells: a systematic review. *PLoS One*. 2016;11:e0151945.
49. Zhang C, Lu Y, Zhou H, et al. Acquiring Kupffer cells in mice using a MACS-based method. *Transplant Proc*. 2015;47:553-557.
50. Poisson J, Plessier A, Kiladjian JJ, et al. French national network for vascular liver, d. (2017) Selective testing for calreticulin gene mutations in patients with splanchnic vein thrombosis: a prospective cohort study. *J Hepatol*;67:501-507.
51. Sørensen KK, Simon-Santamaria J, McCuskey RS, Smedsrød B, (2011) Liver sinusoidal endothelial cells. *Comprehensive Physiology*. John Wiley & Sons, Inc.
52. Strauss O, Phillips A, Ruggiero K, Bartlett A, Dunbar PR. Immunofluorescence identifies distinct subsets of endothelial cells in the human liver. *Sci Rep*. 2017;7:44356.
53. Holt MP, Cheng L, Ju C. Identification and characterization of infiltrating macrophages in acetaminophen-induced liver injury. *J Leukoc Biol*. 2008;84:1410-1421.
54. Krenkel O, Tacke F. Liver macrophages in tissue homeostasis and disease. *Nat Rev Immunol*. 2017;17:306-321.
55. Xie G, Wang L, Wang X, Wang L, DeLeve LD. Isolation of periportal, midlobular, and centrilobular rat liver sinusoidal endothelial cells enables study of zonated drug toxicity. *Am J Physiol Gastrointest Liver Physiol*. 2010;299:G1204-G1210.
56. DeLeve LD. Liver sinusoidal endothelial cells and liver regeneration. *J Clin Invest*. 2013;123:1861-1866.
57. Ichikawa S, Mucida D, Tyznik AJ, Kronenberg M, Cheroutre H. Hepatic stellate cells function as regulatory bystanders. *J Immunol*. 2011;186:5549-5555.
58. Bourgognon M, Klippstein R, Al-Jamal KT. Kupffer cell isolation for nanoparticle toxicity testing. *J Vis Exp*. 2015:e52989.
59. Tatsumi K, Ohashi K, Mukobata S, et al. Hepatocyte is a sole cell type responsible for the production of coagulation factor IX in vivo. *Cell Med*. 2012;3:25-31.
60. Fiani ML, Beitz J, Turvy D, Blum JS, Stahl PD. Regulation of mannose receptor synthesis and turnover in mouse J774 macrophages. *J Leukoc Biol*. 1998;64:85-91.
61. Frankel AE, Fu T, Burbage C, et al. Lectin-deficient ricin toxin intoxicates cells bearing the D-mannose receptor. *Carbohydr Res*. 1997;300:251-258.
62. Wahome PG, Ahlawat S, Mantis NJ. Identification of small molecules that suppress ricin-induced stress-activated signaling pathways. *PLoS One*. 2012;7:e49075.
63. Sandvig K, Olsnes S, Pihl A. Kinetics of binding of the toxic lectins abrin and ricin to surface receptors of human cells. *J Biol Chem*. 1976;251:3977-3984.
64. Baluna R, Ghetie V, Oppenheimer-Marks N, Vitetta ES. Fibronectin inhibits the cytotoxic effect of ricin A chain on endothelial cells. *Int J Immunopharmacol*. 1996;18:355-361.
65. Baluna R, Rizo J, Gordon BE, Ghetie V, Vitetta ES. Evidence for a structural motif in toxins and interleukin-2 that may be responsible for binding to endothelial cells and initiating vascular leak syndrome. *Proc Natl Acad Sci USA*. 1999;96:3957-3962.
66. Baluna R, Coleman E, Jones C, Ghetie V, Vitetta ES. The effect of a monoclonal antibody coupled to ricin A chain-derived peptides on endothelial cells in vitro: insights into toxin-mediated vascular damage. *Exp Cell Res*. 2000;258:417-424.
67. Yermakova A, Klokk TI, O'Hara JM, Cole R, Sandvig K, Mantis NJ. Neutralizing monoclonal antibodies against disparate epitopes on ricin toxin's enzymatic subunit interfere with intracellular toxin transport. *Sci Rep*. 2016;6:22721.
68. Sully EK, Whaley KJ, Bohorova N, et al. Chimeric plantibody passively protects mice against aerosolized ricin challenge. *Clin Vaccine Immunol*. 2014;21:777-782.

69. Fodstad O, Olsnes S, Pihl A. Toxicity, distribution and elimination of the cancerostatic lectins abrin and ricin after parenteral injection into mice. *Br J Cancer*. 1976;34:418-425.
70. Vance DJ, Tremblay JM, Mantis NJ, Shoemaker CB. Stepwise engineering of heterodimeric single domain camelid VHH antibodies that passively protect mice from ricin toxin. *J Biol Chem*. 2013;288:36538-36547.
71. Yermakova A, Klokk TI, Cole R, Sandvig K, Mantis NJ. Antibody-mediated inhibition of ricin toxin retrograde transport. *MBio*. 2014;5:e00995.
72. Rhodes DA, Isenberg DA. TRIM21 and the function of antibodies inside cells. *Trends Immunol*. 2017;38:916-926.
73. Pipirou Z, Powlesland AS, Steffen I, Pohlmann S, Taylor ME, Drickamer K. Mouse LSECtin as a model for a human Ebola virus receptor. *Glycobiology*. 2011;21:806-812.
74. Roy CJ, Brey RN, Mantis NJ, et al. Thermostable ricin vaccine protects rhesus macaques against aerosolized ricin: epitope-specific neutralizing antibodies correlate with protection. *Proc Natl Acad Sci USA*. 2015;112:3782-3787.
75. Smallshaw JE, Firan A, Fulmer JR, Ruback SL, Ghetie V, Vitetta ES. A novel recombinant vaccine which protects mice against ricin intoxication. *Vaccine*. 2002;20:3422-3427.
76. Vitetta ES, Smallshaw JE, Schindler J. Pilot phase IB clinical trial of an alhydrogel-adsorbed recombinant ricin vaccine. *Clin Vaccine Immunol*. 2012;19:1697-1699.
77. Trefts E, Gannon M, Wasserman DH. The liver. *Curr Biol*. 2017;27:R1147-R1151.
78. Kasturirangan S, Rainey GJ, Xu L, et al. Targeted Fcgamma Receptor (FcgammaR)-mediated clearance by a biparatopic bispecific antibody. *J Biol Chem*. 2017;292:4361-4370.
79. Wohlleber D, Knolle PA. The role of liver sinusoidal cells in local hepatic immune surveillance. *Clin Transl Immunol*. 2016;5:e117.
80. Fodstad O, Kvalheim G, Godal A, et al. Phase I study of the plant protein ricin. *Cancer Res*. 1984;44:862-865.
81. Skilleter DN, Paine AJ, Stirpe F. A comparison of the accumulation of ricin by hepatic parenchymal and non-parenchymal cells and its inhibition of protein synthesis. *Biochim Biophys Acta*. 1981;677:495-500.
82. Houston LL. Transport of ricin A chain after prior treatment of mouse leukemia cells with ricin B chain. *J Biol Chem*. 1982;257:1532-1539.
83. Vitetta ES, Thorpe PE. Immunotoxins containing ricin A or B chains with modified carbohydrate residues act synergistically in killing neoplastic B cells in vitro. *Cancer Drug Deliv*. 1985;2:191-198.
84. Rapak A, Falnes PO, Olsnes S. Retrograde transport of mutant ricin to the endoplasmic reticulum with subsequent translocation to cytosol. *Proc Natl Acad Sci USA*. 1997;94:3783-3788.
85. van Deurs B, Sandvig K, Petersen OW, Olsnes S, Simons K, Griffiths G. Estimation of the amount of internalized ricin that reaches the trans-Golgi network. *J Cell Biol*. 1988;106:253-267.
86. van Deurs B, Tonnessen TI, Petersen OW, Sandvig K, Olsnes S. Routing of internalized ricin and ricin conjugates to the Golgi complex. *J Cell Biol*. 1986;102:37-47.
87. Song K, Mize RR, Marrero L, Corti M, Kirk JM, Pincus SH. Antibody to ricin a chain hinders intracellular routing of toxin and protects cells even after toxin has been internalized. *PLoS One*. 2013;8:e62417.
88. Gage E, Hernandez MO, O'Hara JM, McCarthy EA, Mantis NJ. Role of the mannose receptor (CD206) in innate immunity to ricin toxin. *Toxins (Basel)*. 2011;3:1131-1145.
89. Liu W, Tang L, Zhang G, et al. Characterization of a novel C-type lectin-like gene, LSECtin: demonstration of carbohydrate binding and expression in sinusoidal endothelial cells of liver and lymph node. *J Biol Chem*. 2004;279:18748-18758.
90. Shimojima M, Takenouchi A, Shimoda H, Kimura N, Maeda K. Distinct usage of three C-type lectins by Japanese encephalitis virus: dC-SIGN, DC-SIGNR, and LSECtin. *Arch Virol*. 2014;159:2023-2031.
91. Tang L, Yang J, Liu W, et al. Liver sinusoidal endothelial cell lectin, LSECtin, negatively regulates hepatic T-cell immune response. *Gastroenterology*. 2009;137:1498-1508. e1-5.
92. Elvevold K, Smedsrod B, Martinez I. The liver sinusoidal endothelial cell: a cell type of controversial and confusing identity. *Am J Physiol Gastrointest Liver Physiol*. 2008;294:G391-400.
93. Sorensen KK, McCourt P, Berg T, et al. The scavenger endothelial cell: a new player in homeostasis and immunity. *Am J Physiol Regul Integr Comp Physiol*. 2012;303:R1217-30.
94. Hu Z, Shi X, Yu B, Li N, Huang Y, He Y. Structural insights into the pH-dependent conformational change and collagen recognition of the human mannose receptor. *Structure*. 2018;26:60-71. e3.
95. Martinez-Pomares L. The mannose receptor. *J Leukoc Biol*. 2012;92:1177-1186.
96. Anderson CL, Ganesan LP, Robinson JM. The biology of the classical Fcgamma receptors in non-hematopoietic cells. *Immunol Rev*. 2015;268:236-240.
97. Lovdal T, Andersen E, Brech A, Berg T. Fc receptor mediated endocytosis of small soluble immunoglobulin G immune complexes in Kupffer and endothelial cells from rat liver. *J Cell Sci*. 2000;113(Pt 18):3255-3266.
98. Chow SK, Casadevall A. Monoclonal antibodies and toxins–a perspective on function and isotype. *Toxins (Basel)*. 2012;4:430-454.
99. Chow SK, Smith C, MacCarthy T, Pohl MA, Bergman A, Casadevall A. Disease-enhancing antibodies improve the efficacy of bacterial toxin-neutralizing antibodies. *Cell Host Microbe*. 2013;13:417-428.
100. Hiatt A, Pauly M, Whaley K, Qiu X, Kobinger G, Zeitlin L. The emergence of antibody therapies for Ebola. *Hum Antibodies*. 2015;23:49-56.
101. Marzi A, Haddock E, Kajihara M, Feldmann H, Takada A. Monoclonal antibody cocktail protects hamsters from lethal marburg virus infection. *J Infect Dis*. 2018;218:S662-S665.
102. Cheng LW, Stanker LH, Henderson TD, 2nd, Lou J, Marks JD. Antibody protection against botulinum neurotoxin intoxication in mice. *Infect Immun*. 2009;77:4305-4313.
103. Nowakowski A, Wang C, Powers DB, et al. Potent neutralization of botulinum neurotoxin by recombinant oligoclonal antibody. *Proc Natl Acad Sci USA*. 2002;99:11346-11350.
104. Sepulveda J, Mukherjee J, Tzipori S, Simpson LL, Shoemaker CB. Efficient serum clearance of botulinum neurotoxin achieved using a pool of small antitoxin binding agents. *Infect Immun*. 2010;78:756-763.
105. Misharin AV, Morales-Nebreda L, Mutlu GM, Budinger GR, Perlman H. Flow cytometric analysis of macrophages and dendritic cell subsets in the mouse lung. *Am J Respir Cell Mol Biol*. 2013;49:503-510.
106. Roche JK, Stone MK, Gross LK, et al. Post-exposure targeting of specific epitopes on ricin toxin abrogates toxin-induced hypoglycemia, hepatic injury, and lethality in a mouse model. *Lab Invest*. 2008;88:1178-1191.

SUPPORTING INFORMATION

Additional information may be found online in the Supporting Information section at the end of the article.

How to cite this article: Mooney B, Torres-Velez FJ, Doering J, Ehrbar DJ, Mantis NJ. Sensitivity of Kupffer cells and liver sinusoidal endothelial cells to ricin toxin and ricin toxin–Ab complexes. *J Leukoc Biol*. 2019;106:1161–1176. https://doi.org/10.1002/JLB.4A0419-123R